CONTROLLED BASEMAPS FOR MARS 2020 ROVER CANDIDATE LANDING SITES. N. R. Williams[1], H. A. Lethcoe[1,3], L. M. Berger[1,4], M. R. Trautman[1], R. L. Fergason[2], R. E. Otero[1], M. P. Golombek[1]. [1]Jet Propulsion Laboratory, California Institute of Technology, Pasadena, CA 91109 (nathan.r.williams@jpl.nasa.gov); [2]US Geological Survey, Flagstaff, AZ; [3]College of the Canyons, Santa Clarita, CA; [4]Occidental College, Los Angeles, CA.

Introduction: The third landing site workshop for the 2020 Mars Rover mission was held in February 2017 and reduced the number of candidate landing sites down to three: Columbia Hills (-14.5711°N, 175.4374°E), Jezero Crater (18.4386°N, 77.5031°E), and NE Syrtis Major (17.8899°N, 77.1599°E) [1]. During descent, the vehicle will use terrain relative navigation (TRN) to divert around potential hazards via automated localization onto a pre-made onboard map. To navigate around small hazards, TRN requires a high-resolution basemap with minimal distortion and precise image coregistration. Such high precision basemaps will also support mapping of geological units, identification of regions of interest for sample collection, and planning potential traverse routes.

Data and Methods: We control higher resolution images to better-controlled lower resolution datasets to remove artificial offset, rotation, and scaling errors. Our underlying control base is the community standard 128 pixel/degree (~462 m sampling) Mars Orbiter Laser Altimeter (MOLA) global topographic basemap [2] and International Astronomical Union's Mars 2000 coordinate system [3]. For a visible image base, we use 12.5 m/pixel High Resolution Stereo Camera (HRSC) ortho-images [4] that have been corrected for topographic distortions and are well co-registered to MOLA. Stereo images at 6 m/pixel from the Mars Reconnaissance Orbiter (MRO) Context Camera (CTX) [5] have been processed into 20 m elevation posting digital elevation models (DEMs) and 6 m/pixel ortho-rectified visible images by the USGS [6,7]. Similarly, stereo images from the High-Resolution Imaging Science Experiment (HiRISE) are also processed to produce 1 m elevation posting DEMs and 25 cm/pixel ortho-rectified visible images [8].

We use a geographic information system (GIS), specifically ArcGIS, to create 60-80 tie-points between distinct features in each combination of overlapping fine and coarse resolution images, as well as in overlapping portions of adjacent images with comparable resolutions. Illumination and shadows change between images due to variable lighting geometry, so instead we elected to use the circular outlines of small fresh impact crater rims. We first co-register CTX ortho-images to HRSC, and then co-register HiRISE ortho-images to that CTX. The same horizontal tie-points are also applied to each HiRISE and CTX DEM.

In addition to horizontal co-registration, we also perform a vertical correction. During HiRISE DEM generation, HiRISE stereo-derived terrain is roughly tied to the Mars aeroid using MOLA tracks [7], but the sparsity of MOLA tracks often leads to erroneous vertical offsets of up to a few tens of meters at DEM seams. Once we have horizontally controlled the ortho-images and DEMs, we subtract the CTX DEM from each overlapping HiRISE DEM to determine the distribution of any vertical errors. We then fit a plane to the differences using least squares and subtract that fitted offset plane from the HiRISE DEMs to reduce artificial tilts and vertical steps at DEM seams.

Results: We have complete HIRISE and CTX DEM and ortho-image coverage for the Jezero crater (Fig. 1) and NE Syrtis (Fig. 2) candidate landing ellipses. We also have complete CTX DEM and ortho-image coverage for Columbia Hills (Fig. 3), as well as several HiRISE DEMs and ortho-images. A strip in the middle of the Columbia Hills ellipse has not yet been processed into a DEM and ortho-images; however, the portion currently lacking HiRISE topography mainly consists of flat and non-hazardous plains, and a non-ortho-rectified but map-projected visible HiRISE image may be used for terrain analysis until the DEM is processed.

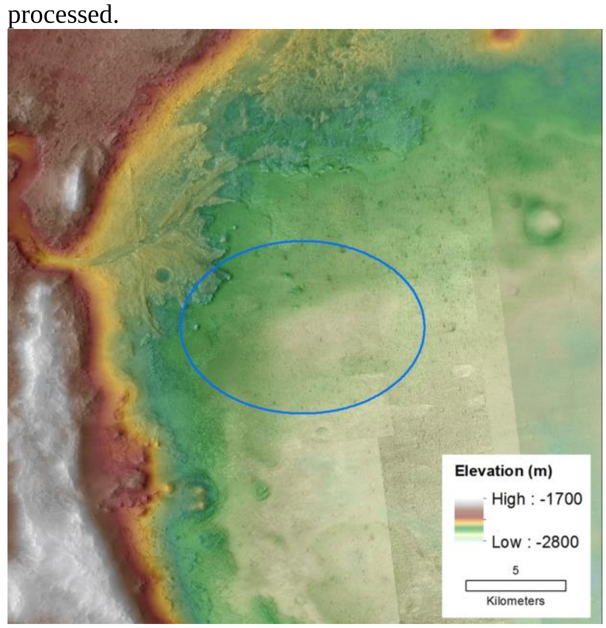

Fig. 1: Jezero Crater candidate landing site with colorized topography over visible images.

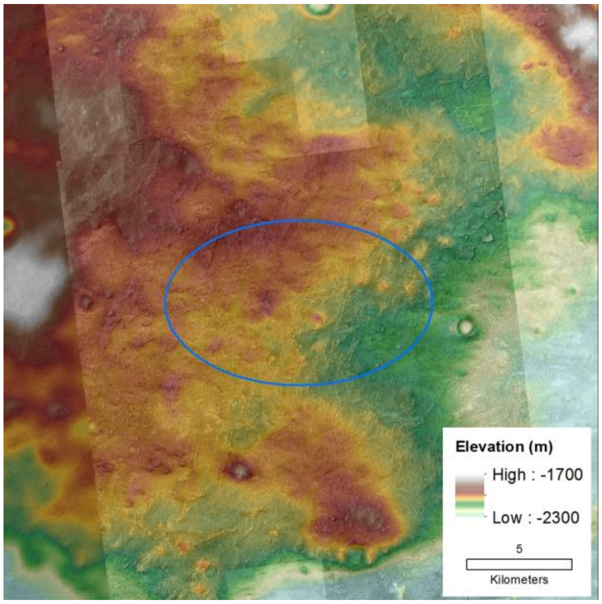

Fig. 2: NE Syrtis candidate landing site with colorized topography over visible images.

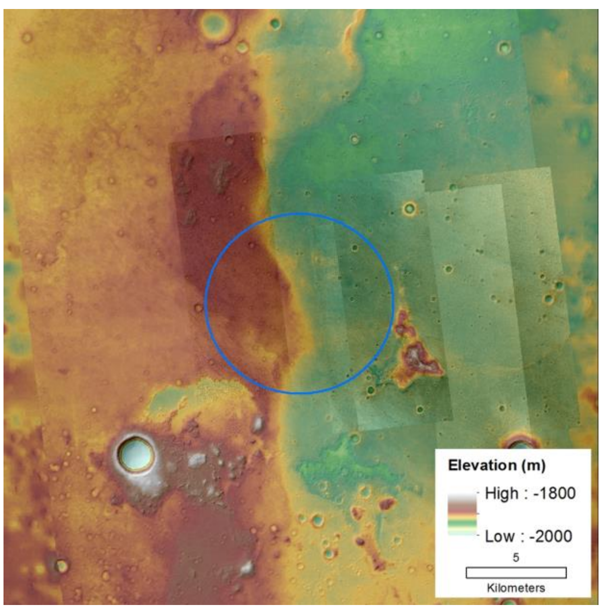

Fig. 3: Columbia Hills candidate landing site with colorized topography over visible images.

Discussion: After performing a first-order transformation to rectify the HiRISE images with their tie-points, we calculated root mean squared (RMS) residual horizontal offsets of 1-5 m for each HiRISE ortho-image relative to the controlled CTX and overlapping co-registered HiRISE images (Fig. 4). We also calculated vertical offsets between overlapping HiRISE DEMs to be <1 m at Columbia Hills and Jezero Crater, and <5 m at NE Syrtis. Vertical offsets between CTX and both MOLA and HiRISE are up to ~20 m primarily in distinct lateral bands orthogonal to the spacecraft azimuth, which we interpret as long-wavelength jitter in the CTX (Fig. 5). Use of multiple additional images in future DEM processing could help correct these jitter errors. Nonetheless, these precise visible image and topographic basemaps have sufficient coverage and small spatial errors to perform engineering analyses, geologic mapping, and science operations planning for the fourth landing site workshop in the second half of 2018.

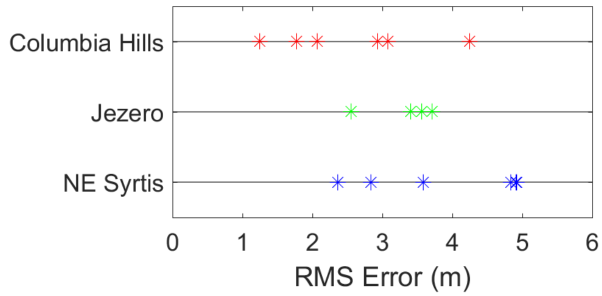

Fig. 4: Root mean squared residual horizontal offsets for each controlled HiRISE ortho-image.

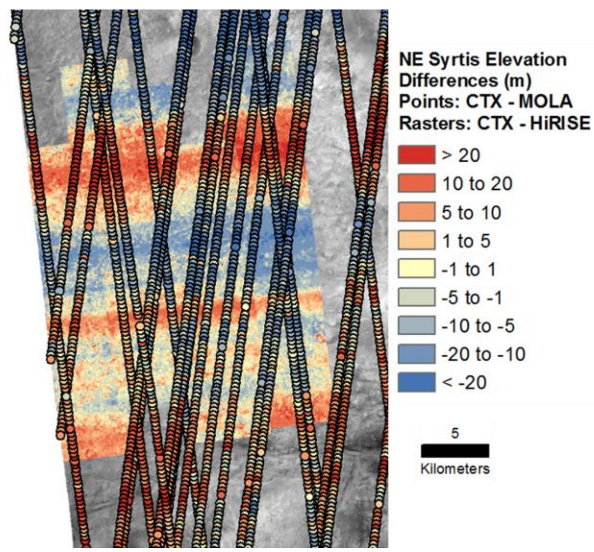

Fig. 5: Residual elevation differences between CTX and MOLA (as points) and between CTX and HiRISE (raster images). The similar banding relative to both implies up to 20 m errors in the CTX, likely from jitter.

References: [1] Golombek M. P. et al. (2018) *LPSC* 49, this issue. [2] Smith D. E. et al. (2001) *JGR* 106, 23689-23722. [3] Seidelmann P. K. et al. (2002) *Celestial Mech. & Dynanical Astronomy* 82, 83-110. [4] Scholten F. et al. (2005) *Photogram. Eng. & Remote Sensing* 71, 1143-1152. [5] Malin M. C. et al. (2007) *JGR* 112, E05S04. [6] Kirk R. L. et al. (2008) *JGR* 113, E00A24. [7] Fergason R. L. et al. (2012) *Space Sci. Rev*. 170, 739-773. [8] McEwen A. S. et al. (2007) *JGR* 112, E05S02.